Full Length Research Paper

Catalytic wet peroxide oxidation of maleic acid: Characterization of copper/micelle templated silica-3-aminopropyltrimethoxysilane and kinetics

Lilian Daniel Kaale

Department of Chemical and Mining Engineering, University of Dar es Salaam (UDSM), P. O. Box 35131, Dar es Salaam, Tanzania.

The study of catalysts enables the catalyst scientist to identify and understand the important steps such as active sites and stages in a catalysts' lifetime. It is thus possible for scientists to design in more rational way, new and efficient catalysts. Therefore, the aim of this study was characterization of copper/micelle templated silica-3-aminopropyltrimethoxysilane (Cu/MTS-AMP) catalyst and study of kinetic parameters of maleic acid in catalytic wet peroxide oxidation. Scanning electron microscope and diffused reflectance infrared Fourier transform spectroscopy were used. SEM pictures of the Cu/ MTS-AMP - pyridine-2-carboxyaldehyde and Cu/ MTS-AMP - 2-hydroxy-1-naphthaldehyde samples show visible differences. The 2-hydroxy-1-naphthaldehyde showed clearly the principal band compared to pyridine-2-carboxyaldehyde. This led to conclusion that the 2-hydroxy-1-naphthaldehyde ligand might be a better choice compared to the pyridine-2-carboxyaldehyde to be used in the preparation of heterogeneous catalysts. However, the catalysts did not show differences in catalytic wet peroxide oxidation of maleic acid. The order of reaction was first order with respect to maleic acid, activation energy E_a, was, 67.052 kJ/mol and pre-exponential factor was 108×10^6 s^{-1}. It was concluded that Cu/ MTS-AMP catalyst was effective for liquid phase oxidation of organic compounds and can be applied for catalytic wastewater treatment systems.

Key words: Catalytic wet peroxide oxidation (CWPO), characterization, copper/micelle templated silica-3-aminopropyltrimethoxysilane (Cu/MTS-AMP), kinetics, wastewater treatment.

INTRODUCTION

Characterization of catalyst

The catalytic wet oxidation (CWO) process is a promising technique for the treatment of highly concentrated or-ganic wastewater that is difficult to degrade biochemically and also it is an environmental friendly method (Masende, et al., 2003; Kaale, 2008; Mdoe et al., 2012; Kaale and Katima, 2013). The process uses oxygen or hydrogen peroxide as oxidant which is made to come into contact with the organic compound in water over a catalyst.

Various heterogeneous catalysts including noble metals and metal oxides have been extensively studied to enhance the efficiency of CWO (Kim and Ihm, 2011). However, it should be kept in mind that, from a global point of view, the recycling of water is not environmentally benign if high energy input technologies are used for this purpose (Eftaxias, 2002; Eftaxias et al., 2006). Thus, the development of efficient wastewater technologies with low energetic and operation costs is essential for all types of wastewater.

While the CWO with application of support metal catalyst seems to be effective for liquid phase oxidation. However, the catalytic wet oxidation (CWO) of wastewater is limited because of the deactivation of metal supported catalysts in aqueous solution (Masende, et al., 2003; Kaale, 2008; Mdoe et al., 2012). Research and development has been performed to find high active and stable catalysts and run these reactions under mild condition (Qiang et al., 2000). The results are not encouraging; as one might expect several completely different set of kinetic parameters for the same complex reaction running at similar reaction conditions (Stanko et al., 2000). One of the main reasons why the reaction kinetic studies have given different results is the leaching of the active sites from the solid surface into the solutions, when applied to liquid-phase reactions. This means that, the catalysts cannot be reused in CWO. The problem of leaching can be avoided or minimized by covalently anchoring the active sites onto the inorganic solids supports (Stanko et al., 2000).

To work on this, it is important to understand the characteristics of both catalyst support and catalyst. The study of catalysts enables the catalyst scientist to identify and understand the important steps e.g. the formation of important reaction, intermediates and activities and stages in a catalysts' lifetime, such as detailed knowledge about catalyst, it is then possible for scientists to design in more rational way, new and efficient catalysts for sustainable production of bulk and fine chemicals as well as for removal of harmful compounds in industrial catalytic processes (Beale et al., 2015).

Five important objectives of catalyst characterization are: 1. to correlate the activity, selectivity, and stability performance of a catalyst in a specific application to its chemical and physical properties in order to design catalysts with optimum performance. 2. Understanding and minimizing catalyst deactivation. 3. Obtaining data for rector and process design such as pore size, strength and morphology of the carrier and location of the active species. 4. Quality control: monitoring changes in chemical and physical properties of a catalyst and 5. Elucidating information on fundamental mechanistic understanding (Bartholomew and Farrauto, 2006).

Scanning electron microscopy (SEM)

The electron microscopy is frequently used to study catalysts, particularly to obtain data about shape, size, crystalline habit, homogeneity, contemporary, presence of amorphous and crystalline (or different crystalline) compounds and their distribution, relative surface of different crystalline faces (Leofanti et al., 1997). Scanning electron microscopy is central to microstructure analysis and therefore important to any investigation relating to the processing, properties, and behaviour of materials that involve their microstructure. The SEM provides information relating to topographical features, morphology, phase distribution, compositional differences, crystal structure, crystal orientation and the presence and location of electrical defects. The strength of the SEM lies in its inherent versatility due to the multiple signals generated, simple image formation process, wide magnification range, and excellent depth of field (Reimer, 2000).

In catalysts based on supported metals only a little fraction of the solid total surface is occupied by the active centre (that is the metal particle) (Leofanti et al., 1997; Reimer, 2000). To understand how a catalyst works, why a sample gives better performance than others or why activity decays by time, the knowledge on the number and on the nature of active sites is crucial. So it is easy to understand why researchers are so interested in surface methods giving data on atomic and molecular levels.

Diffuse reflectance infrared Fourier transform spectroscopy (DRIFTS)

Infrared spectroscopy detects the vibration characteristics of chemical functional groups in a sample. When an infrared light interacts with the matter, chemical bonds will stretch, contract and bend. As a result, a chemical functional group tends to adsorb infrared radiation in a specific wave number range regardless of the structure of the rest of the molecule. For example, the C=O stretch of a carbonyl group appears at around 1700 cm^{-1} in a variety of molecules. Hence, the correlation of the band wave number position with the chemical structure is used to identify a functional group in a sample. It is possible in this way to study interactions of molecules present in the reaction environment and to obtain more direct pieces of information on surface reactivity and reaction mechanism (Leofanti et al., 1997; Thirugnanasambandham and SivaKumar, 2015).

IR spectroscopy can also give direct information on the surface; particularly in the case of oxides: in fact the surface atoms tend to complete their coordination sphere using mainly OH groups, whose stretching vibrations fall in the 3000-4000 cm^{-1} range. Position of bands gives pieces of information on the nature (that is, the acid strength) of hydroxyl group that are often the catalytic active sites. Moreover it is possible to verify the influence on surface sites of probe molecules (Leofanti et al., 1997; Gongshin and Ralph, 2004).

A further use of spectroscopy is to confirm the identity

of a compound by comparison with a known sample. In this instance, rather than looking for a limited number of peaks specific to a particular part of the molecule, infrared spectra are recorded for both the unknown and known compounds. For the compounds to be confirmed as the same, all peaks should match in terms of position and relative intensity. The peaks at higher energy (4000-1000 cm^{-1}) are typical of certain characteristic groups and ligands within molecules and they are used to assign compound to its class, while those at lower energies (typically below 1000 cm^{-1}) are known as the fingerprint region since they are sensitive to small variations between similar compounds.

Therefore, in order to select good catalysts it is important to study parameters of catalysts such as texture because its determination will be able to relate their catalytic activity to their properties. Characterization of catalysts becomes a key point in any study in the field of catalysts. Therefore, the aim of this study was to study the characteristics of copper/micelle templated silica-3-aminopropyltrimethoxysilane catalyst and for this scanning electron microscope (SEM) and diffuse reflectance infrared Fourier transform spectroscopy (DRIFTS) were used. The kinetic parameters of maleic acid using copper/micelle templated silica-3-aminopropyltrimethoxysilane were also studied.

MATERIALS AND METHODS

Catalyst preparation

Preparation of micelle templated silica-3-aminopropyltrimethoxysilane

To a stirred solution of cashew nut shell liquid (CNSL) (2.5 g) in aqueous ethanol (46 ml of absolute ethanol and 54 ml of distilled water) tetraethoxysilane (TEOS, 8.07 g) and 3-aminopropyltriethoxysilane (AMPS, 1.7 g) was added at room temperature separately, but simultaneously and rapidly. The mixture was initially clear, but increasingly became cloudy and after 24 h it was a thick brown paste. After 24 h, the thick solution was filtered and the brown solid was washed with ethanol. The template from the resulting brown powder was removed by Soxhlet method for 5 h. The final powder was then dried in an oven at 100°C overnight.

Preparation of MTS-AMP CNSL supported Schiff base

The prepared MTS-AMP CNSL was further modified with aromatic carbonyl compound in order to form supported Schiff base. Schiff bases can be synthesized from an aromatic amine and a carbonyl compound in a nucleophilic addition to a hemiaminal followed elimination of water to the imine. In order to explore structure-activity relationship of the catalysts the ligands were fine-tuned so as to get diverse structures. Two different, though related, ligands were used namely; pyridine-2-carboxyaldehyde and 2- 2-hydroxynaphthaldehyde.

In a typical preparation, to a stirred solution of the ligand (2-pyridinecarboxaldehyde, or 2-2-hdroxynaphthaldehyde) in an absolute ethanol (50 cm^3 ethanol and 5.46 mmol ligand), the dried MTS-AMP CNSL (2 g) was added slowly and the mixture was refluxed and vigorously stirred for 10 h. After 10 h the reflux was stopped and the Schiff base modified MTS-AMP CNSL (2 g) was filtered under reduced pressure and washed with excess ethanol and dried in an oven at 100°C overnight.

Preparation of copper Schiff base supported on MTS-AMP

The final MTS-AMP CNSL supported copper (II) acetate catalysts were achieved by reacting above support with a solution of copper (II) acetate (2 g) in toluene. The mixture was refluxed for 5 h and the supported catalyst was filtered and washed thoroughly with methanol. The catalyst was then dried over night in air at room temperature. The resulting Cu supported catalyst was conditioned for a total of 6 h by refluxing in ethanol and acetone so as to remove any surface physisorbed copper. The conditioned catalyst was dried overnight at 100°C before characterization step and used in the catalytic wet oxidation (CWO) of maleic acid.

Characterization of copper/micelle templated silica-3-aminopropyltrimethoxysilane

Scanning electron microscopy (SEM)

Scanning electron micrographs were taken using scanning electron microscopy. The different powder samples were placed on aluminum SEM specimen mount stubs from Electron Microscopy Sciences (EMS) using carbon coated conductive adhesive tabs also from EMS. Each sample holder for the Zeiss (LEO) 1530 VP SEM can hold up to eight specimen stubs.

The sample chamber of the SEM was initially under high vacuum (less than 5×10^{-6} Torr). The sample chamber was vented using dry nitrogen gas to facilitate quicker pumpdown. The sample holder with eight samples was attached to the sample stage in the SEM, the chamber was closed and the automatic vacuum pumping system was started. The automatic pumpdown started the mechanical scroll backing pump and the turbo pump. During pumpdown the interior of the sample chamber was observed using TV camera and LEDs as a light source. It was noticed that the powder samples remained on the stubs during pumpdown. The electron gun in this SEM is a Shottky thermally assisted field emission type which has its own vacuum pumps and is isolated from the sample chamber when the sample chamber is opened. The electron gun was always kept on and only the accelerating voltage of the SEM was turned on and off.

When the pressure in the sample chamber was less than 1.5×10^{-5} Torr and the column chamber valve had opened the accelerating voltage was initially set at 3 kV and the in-lens secondary electron detector was selected. The first sample was positioned so that the electron beam would be scanned across it. The image formed by the secondary electrons was observed to have artifacts associated with the sample charging. To reduce the effects of the sample charging the SEM was switched to VP (variable pressure) mode. In VP mode the sample chamber was backfilled with nitrogen gas to a pressure of 30 Pa, the accelerating voltage was set to 25 kV, and the VPSE secondary electron detector was selected. The low pressure nitrogen gas in the chamber acted like an electron conductor and reduced sample charging artifacts.

Images of the samples were formed using secondary electrons from the samples. Secondary electrons are loosely bound electrons in the sample that gain enough energy from the scanned electron beam from the SEM to escape the sample surface. In VP mode these generated secondary electrons are attracted to the VPSE detector by an electrical bias of typically 350 to 380 V. The electron beam from the SEM was slowly scanned across a small area (the size of which depends on the magnification) of the sample and the

secondary electrons that were generated are detected. The images were then saved as computer files.

Diffuse reflectance infrared Fourier transform spectroscopy (DRIFTS)

The FT-IR Spectroscopy (Perkin-Elmer Cooperation) was used and Potassium bromide (KBr) was used as diluents (matrixes) for samples measurements. About 1 mg of the dried sample and 30 mg KBr were finely ground. The powder mixture was then mounted in a sample holder through which the beam of the spectrometer was passed. Measurement and calibration were made at an ambient temperature of approximately 20°C, having allowed the temperature of instrument to stabilize for 20 min with power switched on. The spectra were recorded at room temperature and background spectrum of finely ground anhydrous KBr was subtracted from the spectra.

Inductive coupled plasma-optical emission spectroscopy (ICP-OES)

Catalysts samples were digested using a milestone Ethos 1600 microwave workstation following protocols outlined in EPA method 3051. Approximately 6 ml of 12 N Hydrochloric Acid and 2 ml of 15.8 N Nitric Acid were added to 0.2 g of sample. The mixture was heated up to 180°C in 15 min, kept at 180°C for 25 min, cooled for 2 h using JY 2000 Inductively Coupled Plasma Optical Emission Spectrometer (ICP-OEM). Cu was measured at 324.754 nm. The instrument was calibrated using 4 multi-element standards of known concentrations. The machine drift was monitored using the midrange calibration standard. Three blanks samples were included in the digestion procedure and analyzed along with the samples. The average of the blanks was subtracted from all measured concentrations before applying the dilution factor. Final concentrations were reported in percent.

Performance test

The experiments were conducted in a batch stirred tank reactor (BSTR) in a temperature of 40°C and an atmospheric pressure. A backward pressure of 1.2 MPa was used to facilitate easy sampling from the reactor. The reactor was a 500 ml volume autoclave (Autoclave Engineers, Zipperclave Hastelloy). The reactor set-up is presented in Figure 1.

RESULTS AND DISCUSSION

Scanning electron microscopy (SEM)

SEM is substantially qualitative technique. The advantage is to give a direct view of the carrier (catalyst support), ligand or catalyst itself. The application of SEM can be effective and specifically applicable in various areas of heterogeneous catalysis, especially in the case when usual investigation methods failed (Gizela et al., 2004). Figure 2 shows the micelle templated silica and Aminopropyltrimethoxysilane (MTS-AMP) using cashew nut shell liquid as template. The SEM images clearly show that in particle sizes and morphologies of Cu - catalyst are different (particularly that impregnated in 2-hydroxy-1-naphthaldehyde ligand) to those of templated silicas. The particles have mixed shapes of spherical and irregular (Figure 2).

Figures 3 to 6 show scanning micrographs of ligands used and catalysts. The effect immobilization on grain sizes and shapes is clearly seen in the Figures 3 to 6. There was less destructive of the grain particles in pyridine-2-carboxyaldehyde ligand compared to the 2-hydroxy-1-naphthaldehyde ligand. It can be noticed in Figures 3 to 6 the average particle sizes and the grain shape have changed to more distinct relative to the parent MTS-AMP (CNSL).

SEM pictures of the Cu/ MTS-AMP - pyridine-2-carboxyaldehyde (Figure 4) and Cu/ MTS-AMP - 2-hydroxy-1-naphthaldehyde (Figure 6) samples show visible differences.

The morphology of MTS-AMP catalyst support influences the catalyst activity. The catalyst with well-ordered crystal structure has a good selectivity (Gizela et al., 2004). However, the catalysts were prepared using two different ligands did not influence the catalyst activity though their microstructures were different.

Diffuse reflectance infrared Fourier transform spectroscopy (DRIFTS)

FT-IR Spectroscopy provides information on the structure of molecules on catalyst surface. Figure 7 represents infrared spectra of MTS-AMP, MTS-AMP-2-hydroxy-1-naphthaldehyde and Copper Catalyst. The MTS-AMP was functionalized with ligand in order to form Schiff base functionalized MTS. The success of this reaction was confirmed by changing of spectrum of MTS-AMP. As exemplified in Figure 8, the new spectrum with respect to the parent material shows some changes in the regions where bending vibrations due to the H–N–H and H–C–H occur. This suggests that some molecular changes in the spacer took place. New band at about 1636 cm^{-1} was observed which may be attributed to a C=N stretching vibration (Werner et al., 2001) which is a good marker for studying functional groups and another new bands at 1540 cm^{-1} was also observed, which corresponding to the aromatic ring breathing mode.

The modified support was further converted to MTS-AMP supported copper (II) catalyst by reacting with copper toluene solution. The spectrum of supported copper catalyst showed all of the principal bands for the Schiff base ligand. The band at 1619 cm^{-1} was assigned to C=N stretching vibration of the imine group. The band at 1540 cm^{-1} was assigned to the aromatic ring-breathing mode. The expected C–H stretching bands were visible between 2800 - 3000 cm^{-1}.

Figure 8 shows copper catalyst supported in two different ligands, pyridine-2-carboxyaldehyde and 2-hydroxy-1-naphthaldehyde. The 2-hydroxy-1-naphthaldehyde showed clearly the principal band compared to pyridine-2-carboxyaldehyde. Band at about 1636 cm^{-1} was observed which may be attributed to a
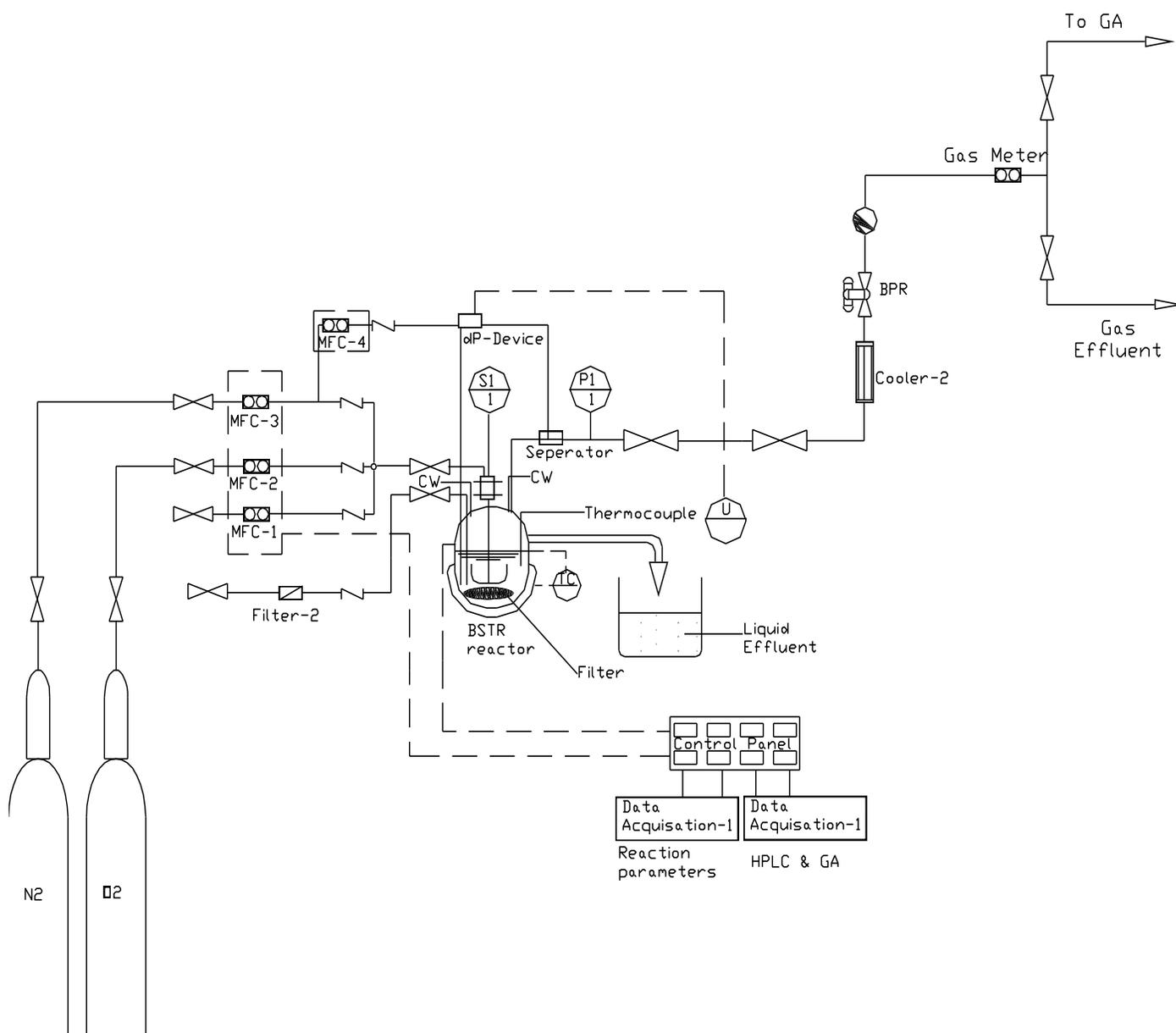
Figure 1. Schematic presentation of the BSTR. BPR: backpressure regulator; CV: on/off valve; d*P*: differential pressure; LI: level indicator; MFC: mass flow controller; PI: pressure indicator; pHI: pH indicator; RV: relief/vent valve; SI: stirrer speed indicator; TC: temperature controller; TI: temperature indicator; WI: weight indicator.

C=N stretching vibration (Smith, 1992). C=N is an imine functional group or chemical compound containing a carbon-nitrogen double bond. This led to conclusion that the 2-hydroxy-1-naphthaldehyde ligand is the best ligand, compared to the pyridine-2-carboxyaldehyde to be used in the preparation of heterogeneous catalysts.

The influence of types of ligand on the degradation of the maleic acid was also studied. The oxidation reaction was studied at Cao= 0.02 g/l; Temperature = 30°C and catalyst = 0.5 g/l. Typical results on the influence of types of ligand on maleic acid degradation are shown in Figure

9. There was no difference between the two ligands used during the catalytic wet peroxide oxidation of maleic acid. In view of the high importance of FTIR spectroscopy for the analysis of the functional group in the samples, it is therefore concluded that the above results are good. FTIR spectroscopy is among the few established (but sometimes disputed) and technically simple methods to analyze functional group (organic group in the samples) in the solid state because it is insensitive to scattering (Wasfi et al., 2002). This can be proved from Figures 7, 8 and 9 FTIR detected the imines group (that is, C=N) and
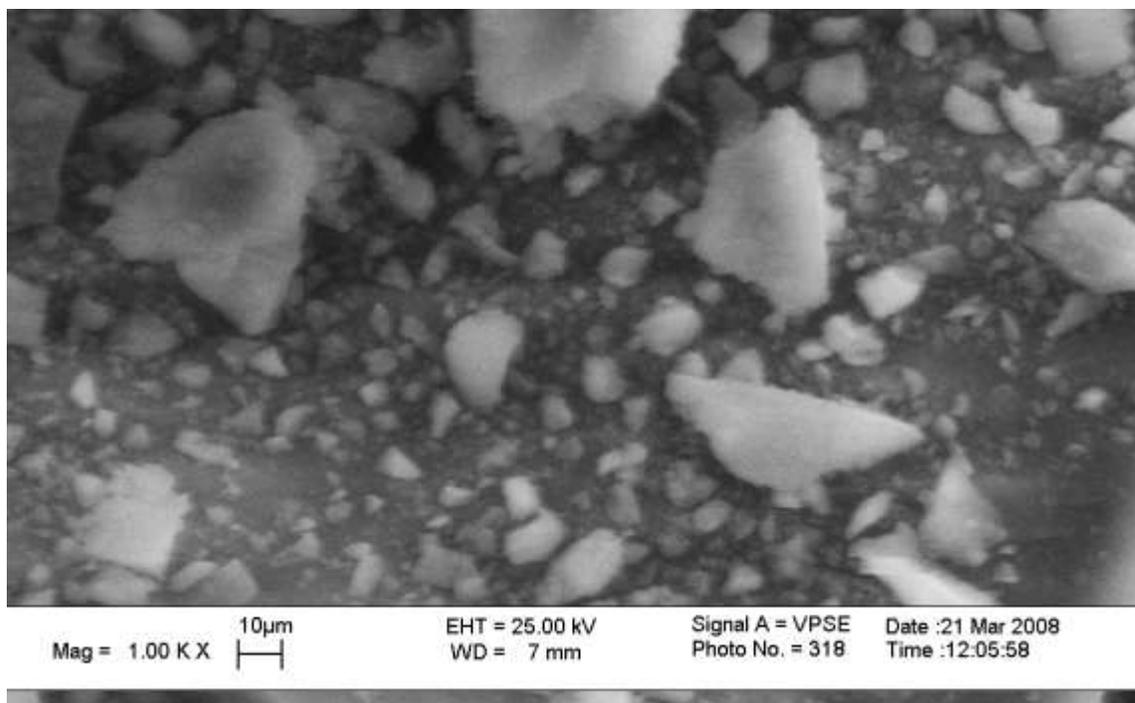
Figure 2. Micelle templated silica-3-aminopropyltrimethoxysilane MTS-AMP on CNSL.
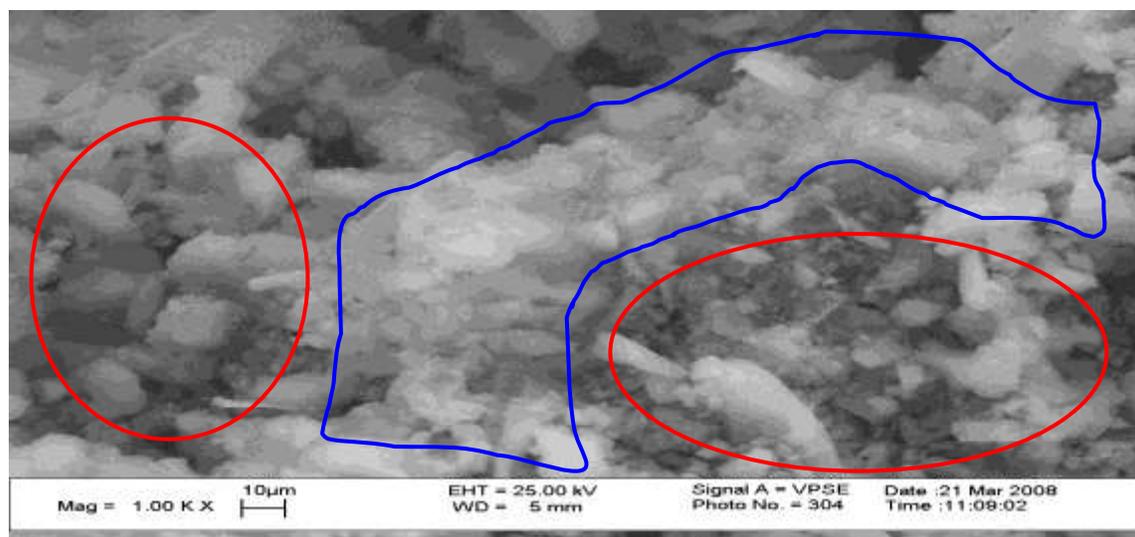
Figure 3. Pyridine-2-carboxyaldehyde ligand on CNSL.

aromatic compound which were supposed to be detected.

Inductive coupled plasma optical emission spectroscopy (ICP-OES)

Inductive coupled plasma optical emission spectroscopy

was used for quantitative determination of copper content on the supported catalysts. The results of the representative samples are as follow. Copper on MST-AMP CNSL support in pyridine-2-carboxyaldehyde had percentage of 5.25, while copper/MTS_AMP CNSL in 2-hydroxy-1-naphthaldehyde had 5.23. Hence, ICP-OES analysis of Cu/MTS-CNSL has discovered the presence of Cu in MTS-CNSL.
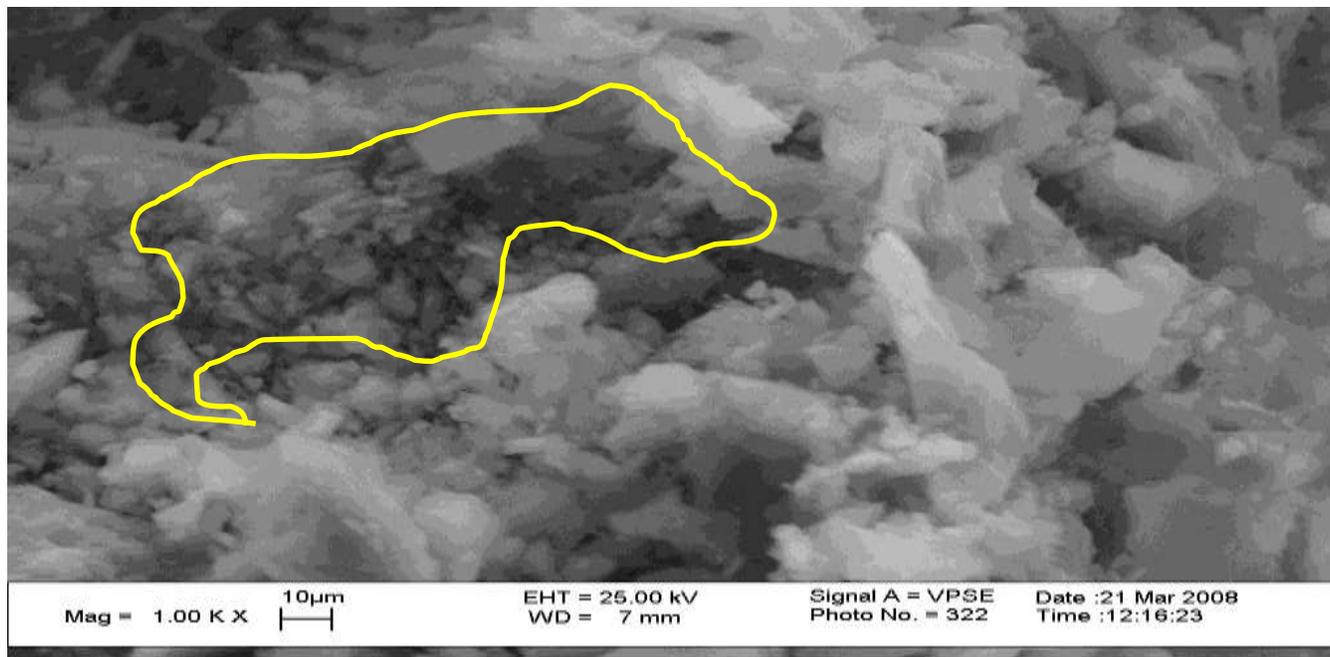
Figure 4. Cu- pyridine-2-carboxyaldehyde CNSL.
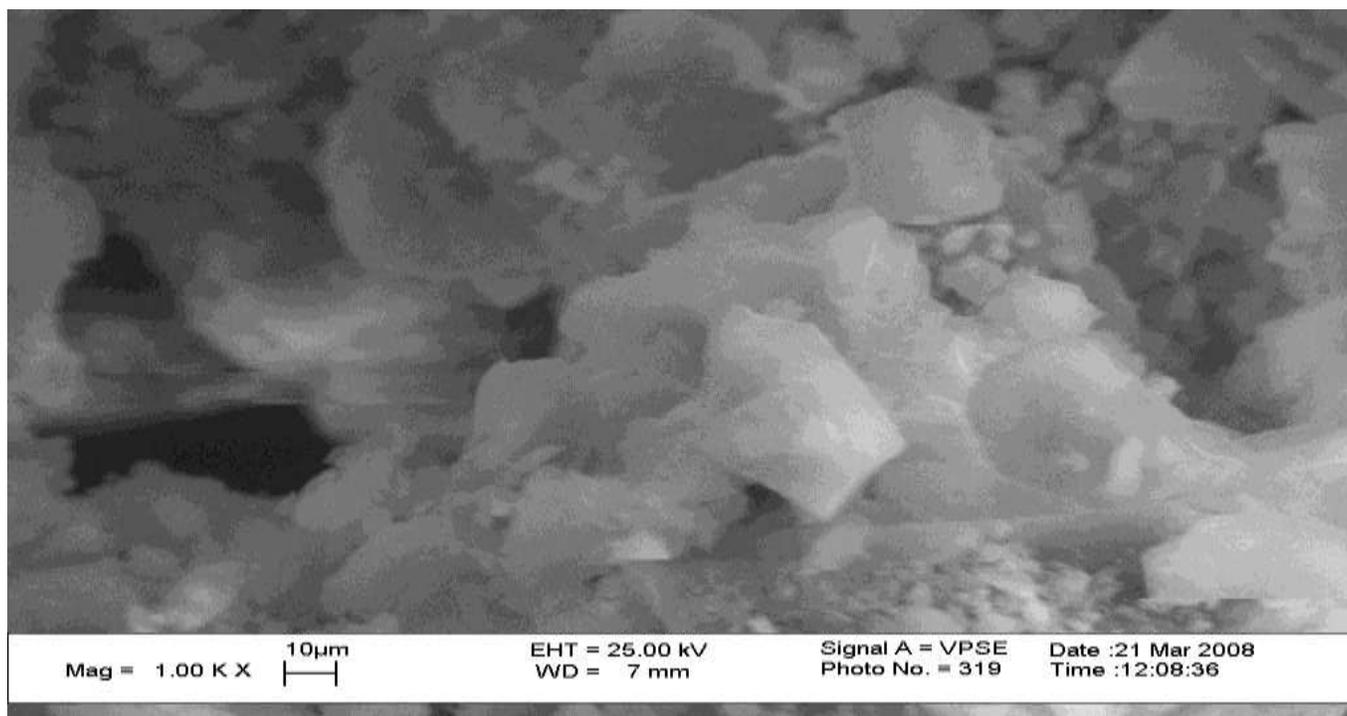
Figure 5. 2-hydroxy-1-naphthaldehyde ligand on CNSL.

Kinetic parameters

Data obtained under a wide range of experimental conditions were used to determine the kinetic parameters; the order of reaction, activation energy and pre-exponential constant. The order of the reaction was
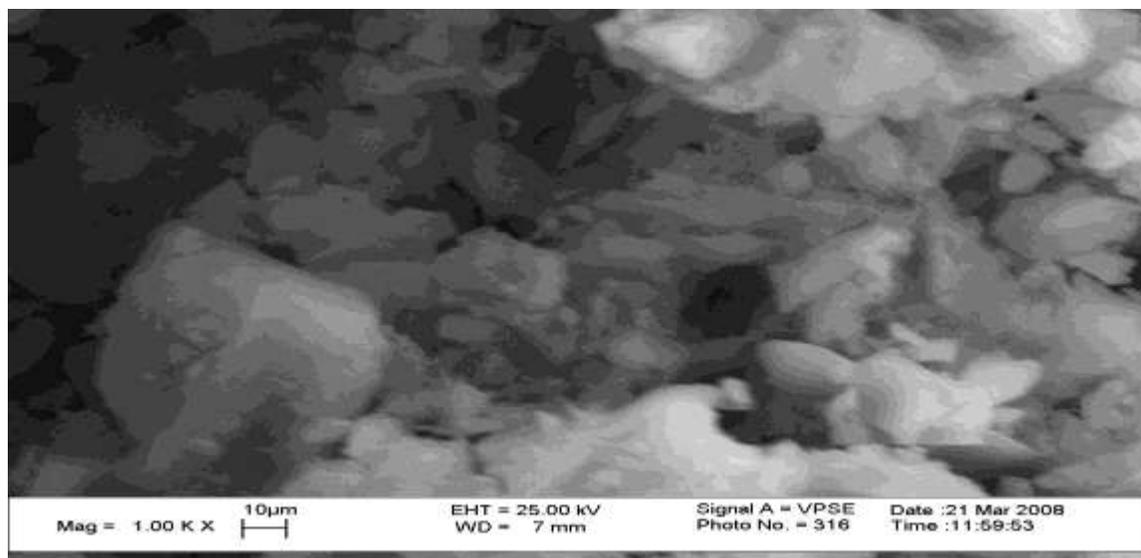
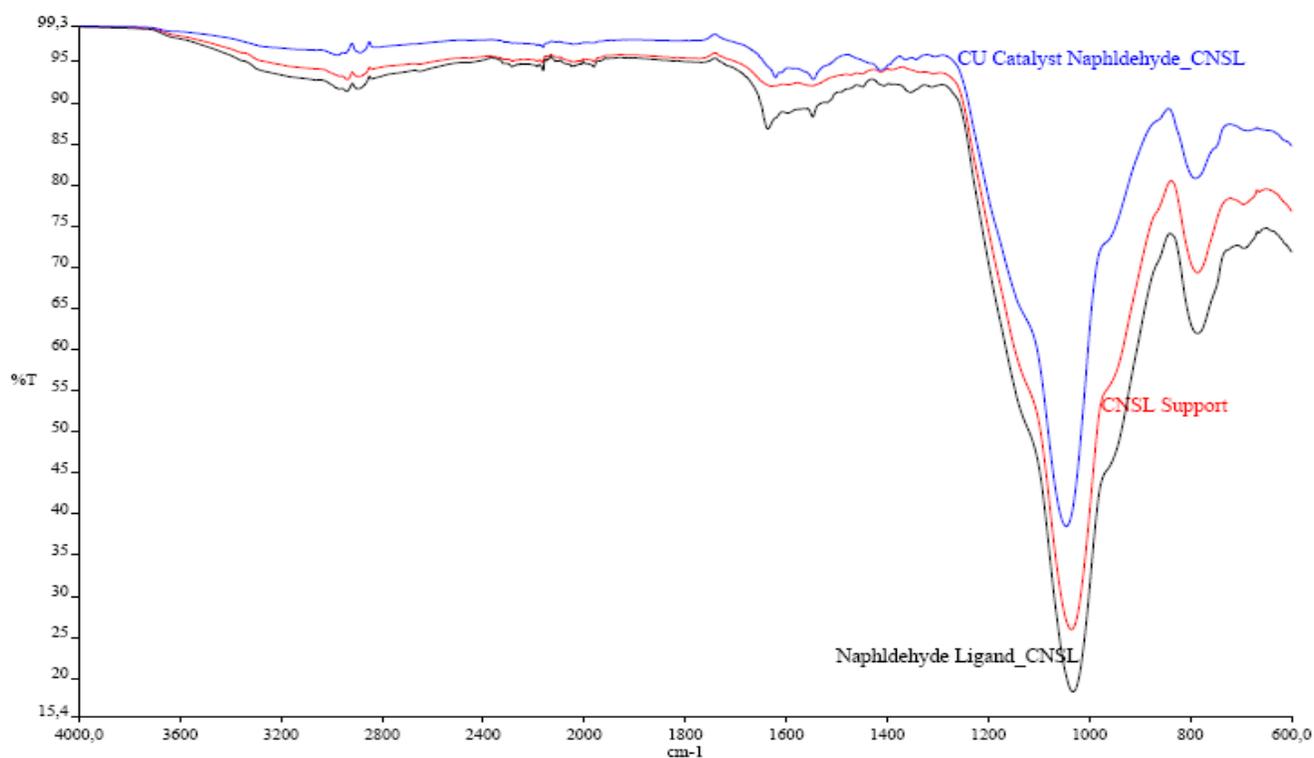**Figure 6.** Cu-2-hydroxy-1-naphthaldehyde ligand on CNSL.

Figure 7. Infrared spectra of MTS-AMP, MTS-AMP-2-hydroxy-1-naphthaldehyde and Copper/ MTS-AMP Catalyst, T = percent transmittance.

determined using integration rate equations. In this method the order was assumed and a graph was drawn for the corresponding integrated rate equation. This procedure was repeated until the order that gave the best fitting was found. The rate equation obtained was for a first order reaction n=1. This value is similar to the previous literature as reported by Kumar et al. (2007) using heterogonous catalysts Co: Bi and Mn: Ce, and Javier et al. (1999) using platinum catalyst.
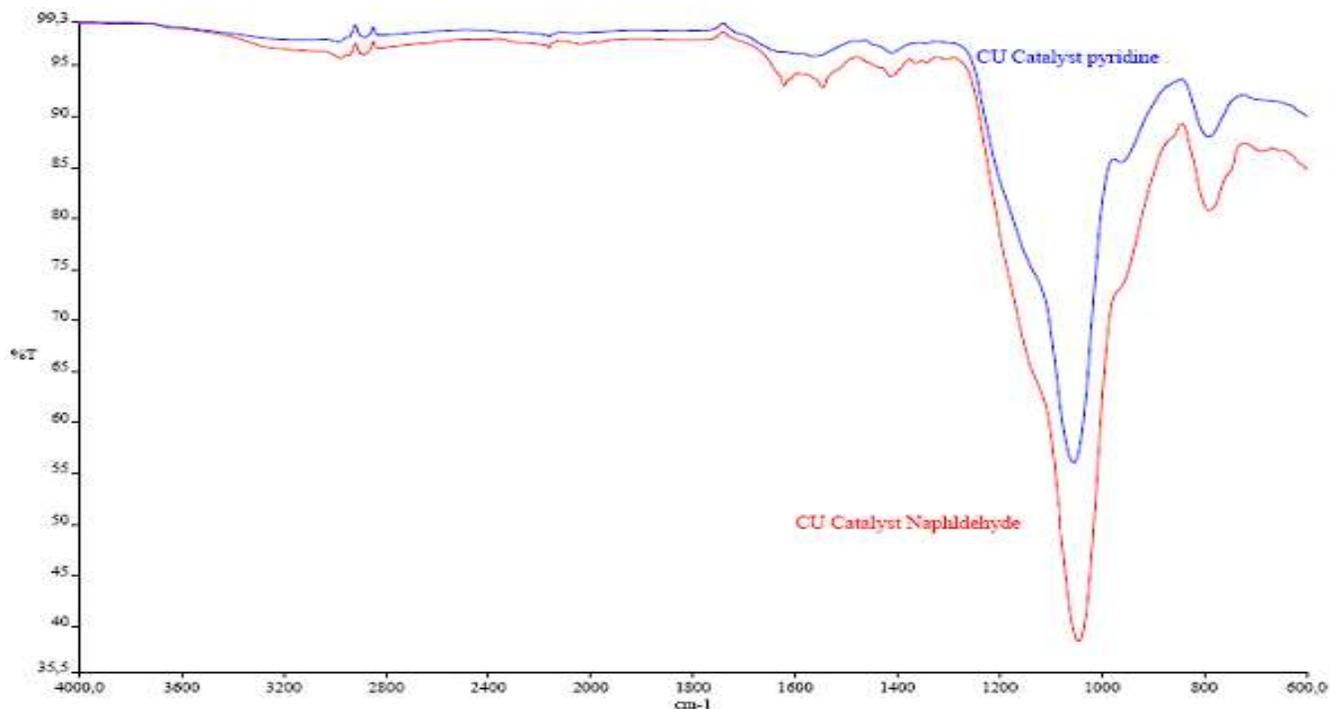
The rate constant, k was also determined using the

Figure 8. Copper catalysts supported in pyridine-2-carboxyaldehyde and 2-hydroxy-1-naphthaldehyde.
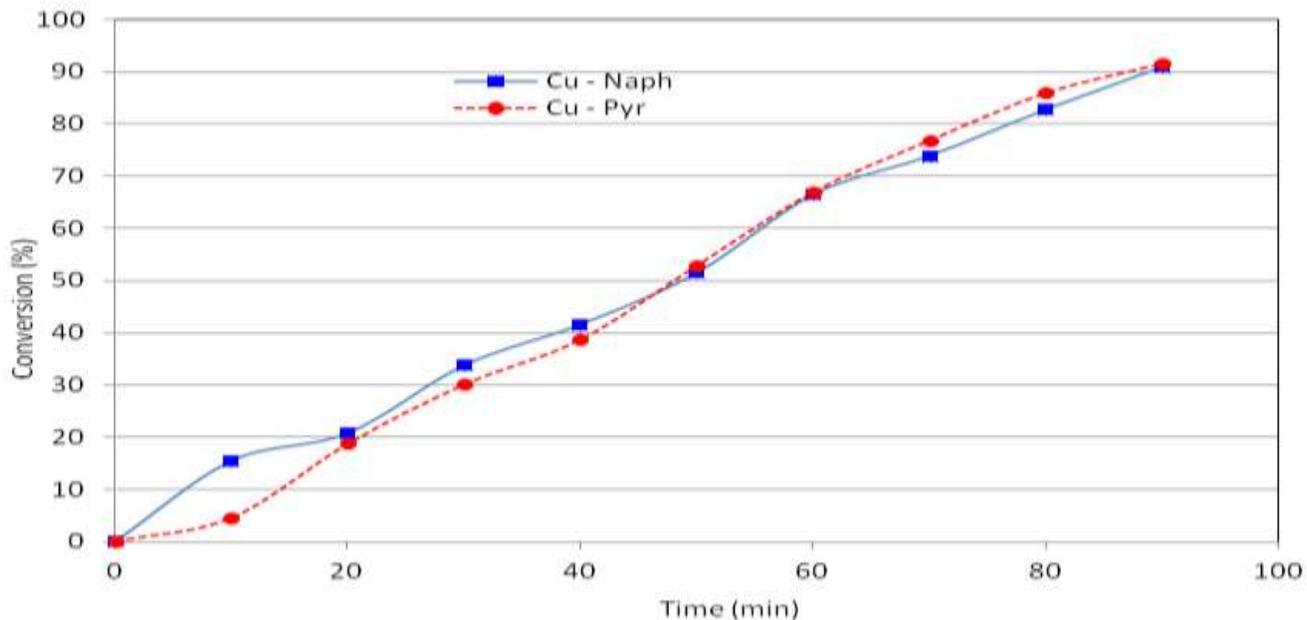

Figure 9. Effect of types of ligands in CWPO of maleic acid: Naph = 2-hydroxy-1-naphthaldehyde and Pyr = pyridine-2-carboxyaldehyde.

slopes of the graph drawn to obtain order of the reaction. Rate constants are fundamental kinetic parameters, for bulk systems and their evaluation is of special concern to the kineticist. The values of k, were changing with temperature which means that it is temperature dependent; $k_{20°C} = 1x10^{-4}$, $k_{30°C} = 4x10^{-4}$, $k_{40°C} = 7x10^{-4}$, and $k_{50°C} = 14x10^{-4}$.

Using experimental results obtained above, k' was
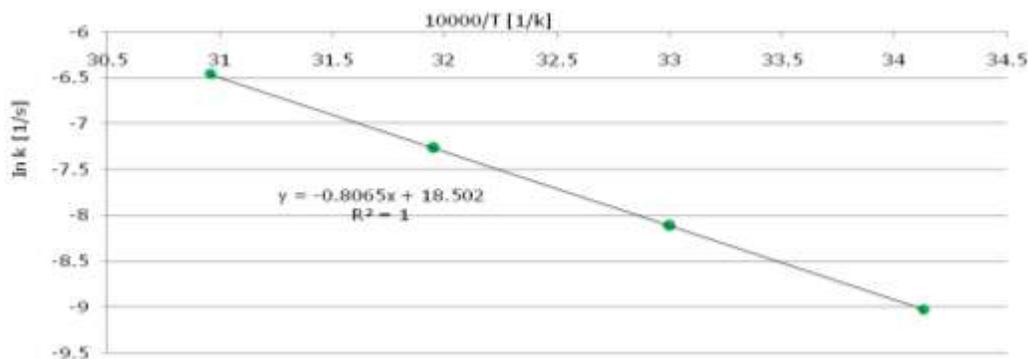
Figure 10. A plot of natural log of rate constant, k' for reaction at different temperatures versus the inverse of temperature in Kelvin with a slope equal to - E_a/R.
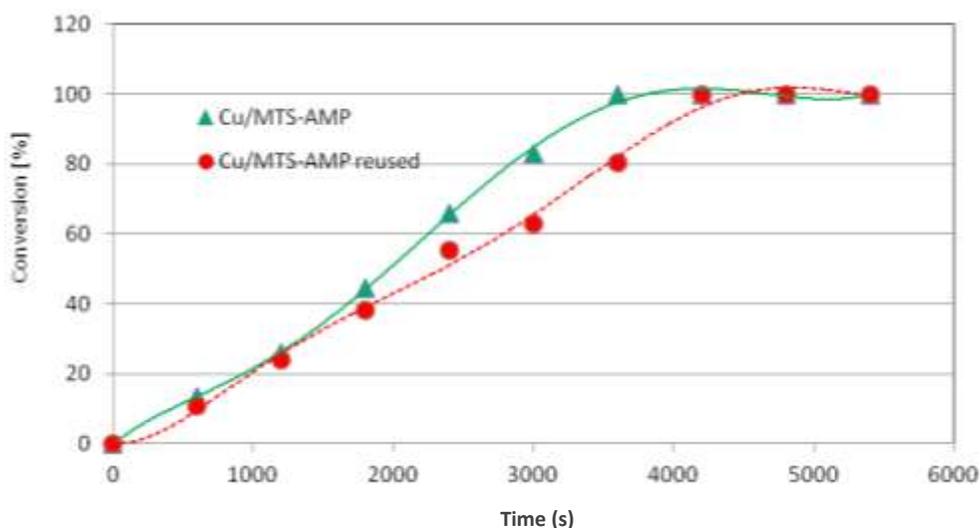
Figure 11. Conversion of maleic acid. Temperature was at 40°C and a catalyst concentration of 0.5 g/l. The solid line fresh catalyst; dotted lines the catalyst was separated from suspension, washed, dried and repeatedly used (5 times) for the oxidation of the maleic acid. Conditions: C_{ma} = 0.01.

evaluated at different temperatures for catalyst Cu- MTS-AMP CNSL. A subsequent Arrhenius representation of k' allowed the calculation of the apparent activation energy for the heterogeneous reaction. Arrhenius equation gives the dependence of the rate constant k, of chemical reactions on the temperature T (in Kelvin) and activation energy E_a.

A plot of natural log of rate constant, k for reaction at different temperatures versus the inverse of temperature in Kelvin with a slope equal to - E_a/R was developed (Figure 10).

Slope × R (gas constant) = 8065 K × 8.314 J/mol

Ea = 67052.41 J/mol = 67.052 kJ/mol

Therefore, the activation energy, E_a = 67.052 kJ/mol. This

value is in agreement with the results reported by Alzaydien (2005) and Javier et al. (1999), 62±5 kJ/mol (over nickel catalyst) and 66.7 kJ/mol (over platinum catalyst) respectively, for maleic acid oxidation.

Pre-exponential factor, A = y-intercept of the above graph = $e^{18.502}$ = 108×10^6 s^{-1}

Stability test of the catalyst

The performance of catalyst in this study is the same as that reported by Kaale (2008); Kaale and Katima (2009) (Figure 11). However, in this study characteristics and kinetic parameters were studied while (Kaale, 2008: Kaale and Katima, 2009) analysed CWPO of maleic acid
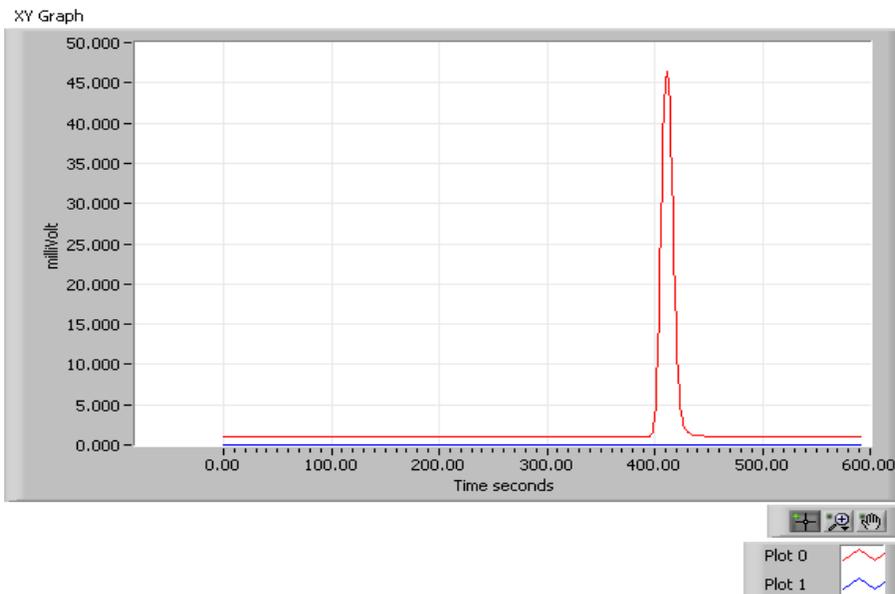
Figure 12. Chromatograph peaks taken immediately before reaction conditions.
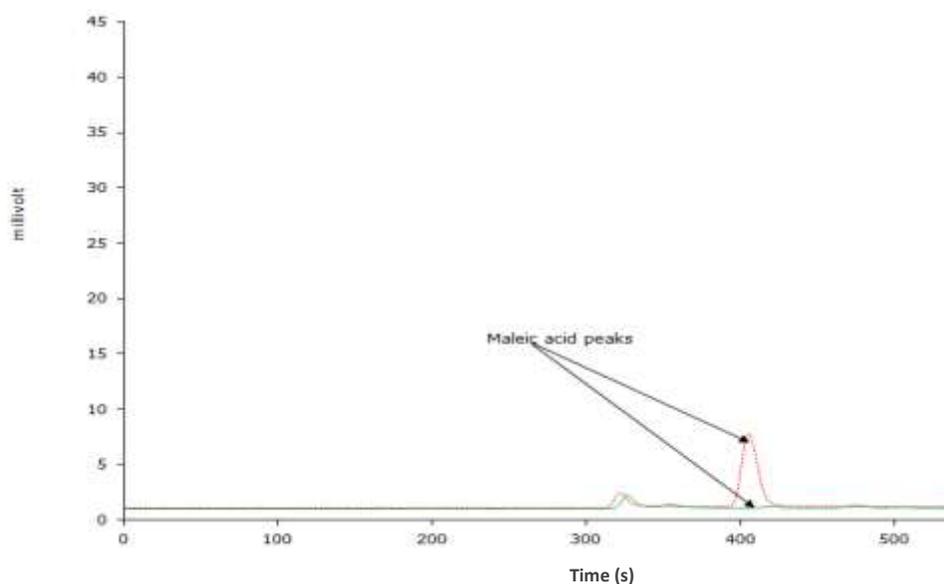
Figure 13. Chromatograph peaks of maleic acid. Temperature was at 40°C and a catalyst concentration of 0.5 g/l. The solid line (green) fresh catalyst; dotted line (read) the catalyst was separated from suspension, washed, dried and repeatedly used (5 times) for the oxidation of the maleic acid. Conditions: $C_{ma} = 0.01$.

at different conditions using Cu- MTS-AMP.

The stability test performed, fresh and reused catalysts were tested. The results obtained of this catalyst were very good, since the maleic acid conversion after one hour was 100 and 80.26% for the first and 5 times reused catalyst, respectively. The results suggest that the reused catalyst is relatively stable. The result was further proved by using peaks of maleic acid obtain from high performance liquid chromatography (HPLC) during analysis of the data. The reused copper catalyst degraded maleic acid in such way that maleic acid peak is almost a quarter of the original peak (Figure 12), while for the fresh catalyst maleic attained 100% conversion after one hour of the reaction (Figure 13).

This further proves that the catalyst is stable and can be used both in liquid phase oxidation of organic compounds

and for catalytic wastewater treatment systems.

Conclusions

Copper/micelle templated silica-3-aminopropyltrimethoxysilane was successfully prepared, characterized and tested. SEM pictures of the Cu/ MTS-AMP - pyridine-2-carboxyaldehyde and Cu/ MTS-AMP - 2-hydroxy-1-naphthaldehyde samples show visible differences. The 2-hydroxy-1-naphthaldehyde showed clearly the principal bands compared to pyridine-2-carboxyaldehyde. This led to conclusion that the 2-hydroxy-1-naphthaldehyde ligand might be a better choice compared to the pyridine-2-carboxyaldehyde to be used in the preparation of heterogeneous catalysts. However, the catalysts did not show differences in catalytic wet peroxide oxidation of maleic acid.

The order of reaction was first order with respect to maleic acid, activation energy Ea, was, 67.052 kJ/mol and pre-exponential factor was 108×10^6 s^{-1}. It was concluded that Cu/ MTS-AMP catalyst was effective for liquid phase oxidation of organic compounds and can be applied for catalytic wastewater treatment systems.

Conflict of Interests

The author has not declared any conflict of interests.

REFERENCES

Alzaydien AS (2005). Kinetics of maleic acid hydrogenation over skeleton nickel in aqueous solutions. J. Appl. Sci. 5:182-186.

Bartholomew CH, Farrauto RJ (2006). Fundamental of industrial catalytic process, 2nd ed. Wiley, J and Sons, Inc. Hoboken, New Jersey.

Beale AM, Stavitski ES, Weckhuysen BM (2015). Characterization of catalysts: Surface and in-situ methods. Encyclopedia of life support systems (EOLSS). Available at: http://www.eolss.net/sample-chapters/c06/e6-190-13-00.pdf   Retrieved on 29/04/2015.

Eftaxias A (2002). Catalytic Wet air oxidation of phenol in a trickle bed reactor: Kinetics and reactor modelling. PhD thesis in Chemical Engineering, University of Virgili University.

Eftaxias A, Font J, Fortuny A, Fabregat A, Stuber F (2006). Catalytic wet air oxidation of phenol over active carbon catalyst Global kinetic modelling using simulated annealing. Appl. Catal. B: Environ. 67:12-23.

Gizela AL, Kiš EE, Bošković GC, Marinković-Nedučin RP (2004). Application of scanning electron microscopy in catalysis. Acta Period. Technol. 35:67-77.

Gongshin Q, Ralph TY (2004). Characterization and FTIR Studies of MnOx-CeO2 Catalyst for Low-Temperature Selective Catalytic Reduction of NO with NH$_3$. J. Phys. Chem. B 108(40):15738-15747.

Javier R, Stan TK, Fernando JB, David BM (1999). Degradation of maleic acid in wet oxidation environment in the presence and absence of platinum catalyst. J. Appl. Catal. B: Environ. 22(4):279-291.

Kaale LD (2008). Kinetic study of catalytic wet peroxide oxidation of maleic acid using heterogeneous catalysts. M.Sc. Thesis, University of Dares Salaam.

Kaale LD, Katima JHY (2013). Performance of activated carbons in the catalytic wet peroxide oxidation (CWPO) of maleic acid. J. Eng. Technol. Res. 5(6):189-199.

Kaale LD, Katima JHY (2009). Factors influencing catalytic wet peroxide oxidation of maleic acid in aqueous phase over copper/micelle templated silica-3-aminopropyltrimethoxysilane catalyst. Water Sci. Technol. 60:2621-2627.

Kim K-H, Ihm S-K (2011). Heterogeneous catalytic wet air oxidation of refractory organic pollutants in industrial wastewaters: A review. J. Hazard. Mater. 186:16-34.

Kumar P, Raghavendra PVK, Chand S (2007). Catalytic wet air oxidation of carboxylic acid present in wastewater. J. Sci. Ind. Res. 65(10):838-842.

Leofanti G, Tozzola G, Padovan M, Petrini G, Bordiga S, Zecchina A (1997). Catalyst characterization: characterization techniques. Catal. Today 34:307-327.

Masende ZPG, Kuster BFM, Plasinski KJ, Janssen FJJD, Katima JHY, Schouten JC (2003). Platinum catalyzed wet oxidation of phenol in a stirred slurry reactor. Practical operation window. J. Appl. Catal. B: Environ. 41:247-267.

Mdoe JEG, Minja RJA, Kaale LD (2012). Wet Oxidation of Maleic Acid by a Pumice Supported Copper (Li) Shiff Base Catalyst. Tanzan. J. Sci. 38(2):28-38.

Qiang W, Xijun H, Po lock Y, Xiu SZ, Gao QL (2000). Copper MCM-41 as catalyst for the wet oxidation of phenol. J. Appl. Catal. B: Environ. 32(3):151-156.

Reimer L (2000). Scanning Electron Microscopy: Physics of Image Formation and Microanalysis, Second Edition. Meas. Sci. Technol. 11:1826.

Smith K (1992). Solid Supports and Catalysts in Organic Reactions, Ellis Horwood Ltd, Chichester.

Stanko H, Ursa OK, Boris O, Antono SA, Hasuck K (2000). Catalytic Wet Oxidation of pheniland other organic pollutants. J. Appl. Catal. B: Environ. 28:113-125.

Thirugnanasambandham K, Sivakumar V (2015). Modeling and optimization of treatment of milk industry wastewater using chitosan–zinc oxide nanocomposite. Desalination Water Treat. pp. 1-9.

Wasfi A, Emil P, Ferrer A, Qing YH (2002). Structure of poly (ethylene glycol-modified horseradish peroxidase in organic solvents: Infrared amide I spectral changes upon protein dehydration are largely caused by Protein Structural Changes and Not by Water Removal Per Se. Biophys. J. 83:3637-3651.

Werner U, Jens M, Neumüller B (2001). The hydrogallation of C=N double bonds - reactions of GaH3·NMe2Et with tetramethyl-2, 3-diazabutadiene. J. Organomet. Chem. 634(2)193-197.